DE GRUYTER
OPEN

Magnetic transformation in Ni-Mn-In Heusler alloy

Marian Kuzma,
Wojciech Maziarz,
Ireneusz Stefaniuk

Abstract. Magnetic properties of a $Ni_{50}Mn_{35.5}In_{14.5}$ Heusler ribbon were studied by ferromagnetic resonance (FMR) in the temperature range of 335–100 K. In the temperature region of 265–170 K, the FMR signal disappeared, in spite of the fact that this region comprised the main crystal transformation temperatures: M_s, M_f, A_s, A_f. In the austenite crystal state, a weak antiferromagnetic interaction was observed, whereas ferromagnetism was detected in the low temperature martensitic state.

Key words: Heusler alloy • Ni-Mn-In • ferromagnetic resonance

M. Kuzma✉, I. Stefaniuk
Faculty of Mathematics and Natural Sciences,
University of Rzeszow,
1 Pigonia Str., 35-959 Rzeszow, Poland,
E-mail: kuzma@ur.edu.pl

W. Maziarz
Institute of Metallurgy and Materials Science
of the Polish Academy of Science,
25 Reymonta Str., 30-059 Krakow, Poland

Introduction

Nonstoichiometric Heusler alloys Ni-Mn-Z (Z = In, Sn, Sb, Ga) show a unique structural austenitic-martensitic phase transition (MPT) driven by the magnetic degrees of freedom [1–3]. The martensitic-austenitic and austenitic-martensitic phase transitions start at temperatures M_s and A_s, respectively, and they are finished at temperatures M_f and A_f, respectively. For $Ni_{49.1}Mn_{35.4}In_{15.5}$, these temperatures are $M_s = 250$ K, $M_f = 219$ K, $A_s = 220$ K, $A_f = 260$ K. The Curie temperatures of these two phases are $T_C^A = 310$ K, $T_C^M = 205$ K for austenite and martensite, respectively [4].

The magnetocaloric effect [5, 6] is related to MPT. It has been suggested that this should be applied in ecological magnetic refrigeration. Ni-Mn-In and Ni-Co-Mn-In alloys seem to offer a new perspective for the optimization of the magnetocaloric effect within the Heusler group of materials [7–9]. However, the MPT is observed at great nonstoichiometry $x > 0.32$, at $Ni_2 Mn_{1+x}In_{1-x}$ [2].

As in all ferromagnetic Ni-Mn Heusler alloys, a sudden drop in the temperature dependence of magnetization is observed as the temperature decreases just below the M_s temperature. Such a drop occurs for small magnetic fields (e.g. 5 mT), as well as for high fields, such as 5T (except in NiMnGa) [4]. The drop in $M(T)$ is caused by the antiferromagnetic correlations below $T < M_s$ [4]. Above M_s, the correlations are ferromagnetic in nature. In fact, below M_s, there are mixed ferromagnetic and anti-

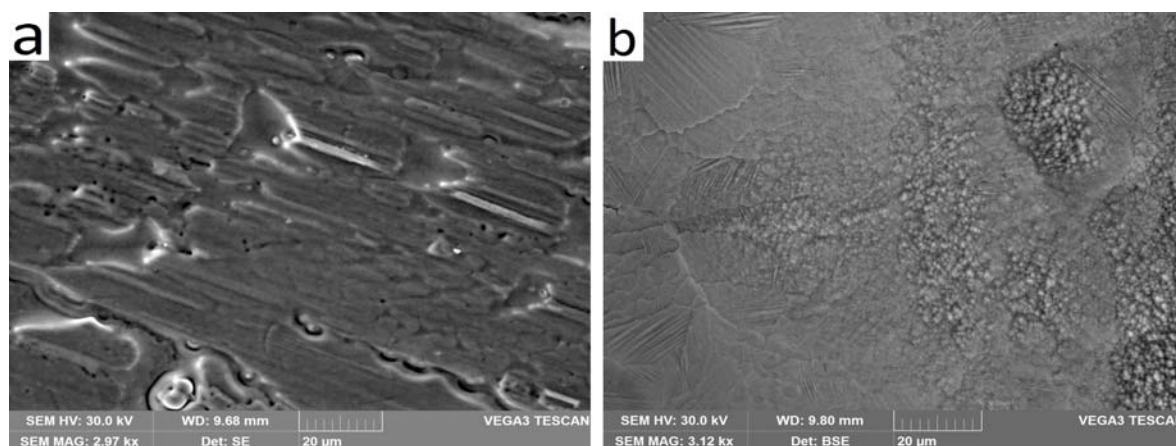**Fig. 1.** SEM micrographs of $Ni_{50}Mn_{35.5}In_{14.5}$ ribbon: morphology of the W side (wheel side) (a), morphology of the F side (free side) (b).

ferromagnetic states. The ferromagnetic resonance technique (FMR) has been applied by us to study such magnetic correlations in a $Ni_{50}Mn_{35.5}In_{14.5}$ ribbon. The same methodology was previously used for a $Ni_{49.1}Mn_{35.4}In_{15.5}$ alloy sample [4].

Experimental

The $Ni_{50}Mn_{35.5}In_{14.5}$ alloy was prepared by induction melting under argon atmosphere using pure elements of 99.9% purity. The melt-spun ribbon of this alloy was formed according to the procedure described in [10, 11]. The structure of the ribbon flakes was the single phase of a 14M modulated monoclinic martensite [10]. The morphology and composition was controlled by scanning electron microscopy (SEM) using a Vega Tescan electron microscopy equipped with the energy-dispersive X-ray (EDX) system.

The magnetic properties of the samples were obtained from the FMR data measured on an X-band Bruker spectrometer (9.43 GHz) in the temperature range of 100–335 K. The magnetic field was perpendicular to the surface of the sample. Resonance spectra were recorded as a function of temperature on decreasing temperature (with a 5 K step) up to 100 K.

Results

In Fig. 1, we present the SEM morphology of two surfaces W and F of the $Ni_{50}Mn_{35.5}In_{14.5}$ sample having a shape of ribbon. The surface W had a contact with wheel of equipment for ribbon fabrication. The surface F shows upper ('free') side. The morphology of these two surfaces differs considerably. The first surface consists of columns of diameter of 10–20 μm disposed parallel to the surface. The F surface is composed of grains. The microstructure of grains is of two types: a plate-like phase associated with martensitic phase, and a high dispersive granular phase with grains of diameter of 1 μm.

The temperature dependence of the ferromagnetic resonance (FMR) spectra is collected in Fig. 2.

The shape of the electron paramagnetic resonance (ESR) spectra is of a Dyson type, with a

great asymmetry parameter of the resonance line $A/B = 2.48$ at room temperature, where A and B are amplitudes of the low field and high field halves of the spectrum, respectively. The temperature dependence of the resonance lines indicates that in the temperature range of 270–150 K the resonance lines are very wide or disappear altogether. Therefore, we study the resonance signal separately, in two temperature regions: 335–265 K and 175–100 K. The temperature dependence of the resonance field B_r and the linewidht ΔB for these two groups of lines are presented in Fig. 3.

Discussion

The characteristic magnetic and structural transition temperatures obtained for an alloy whose composition was very close to our $Ni_{49.1}Mn_{35.4}In_{15.5}$ sample [4] are collected in Fig. 4. The range of the temperatures in which the resonance signal is not observed is marked in Fig. 4 as well. This range contains all the structural transition temperatures M_s, M_f, A_s, A_f. The magnetic transition temperatures lie outside of this range of temperature (T_C^A is close to the border, i.e., to the M_f). Therefore, we conclude that the high temperature magnetic resonance (MR) signal origins from a pure austenitic phase, whereas the low temperature MR signal belongs to the pure martensitic phase. This is an extraordinary result in
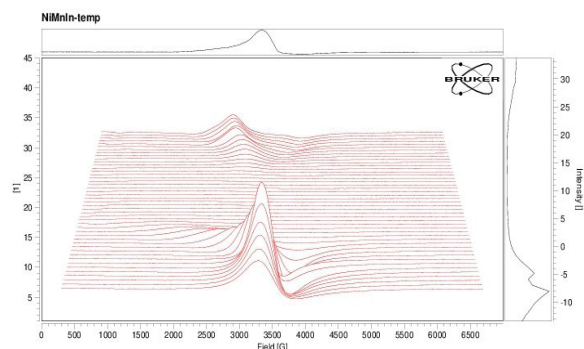

Fig. 2. Temperature dependence of ESR spectra of $Ni_{50}Mn_{35.5}In_{14.5}$. The first line is recorded at temperature 335 K, the consecutive lines are recorded with gradually decreasing temperature with step of 5 K. The last line (upper) relates to 100 K .
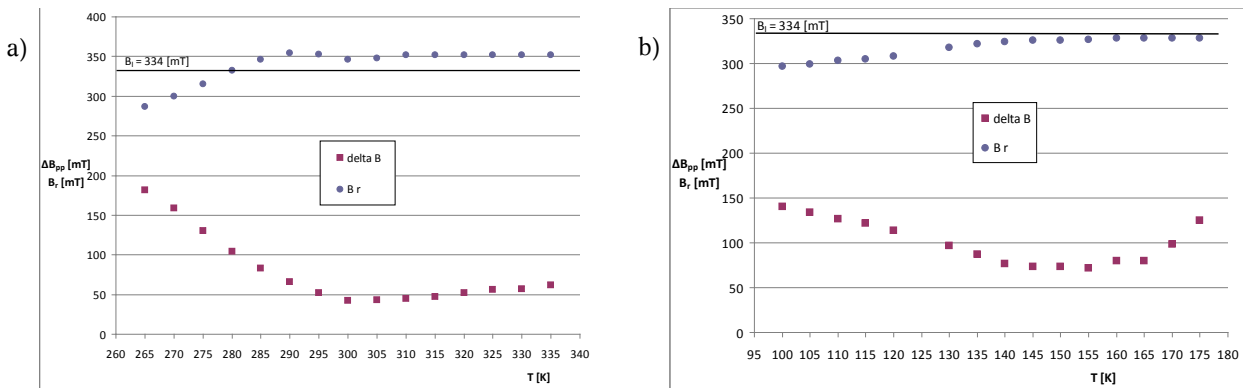
Fig. 3. Temperature dependence of the resonance field B_r, and linewidth ΔB_{pp}, of $Ni_{50}Mn_{35.5}In_{14.5}$ in two regimes of temperatures.

that the mixed phases do not exhibit any magnetic interactions in the MR measurements.

The isotropic resonance field $B_I = \omega/\gamma$ (ω is the microwave frequency, $\omega = 2\pi\nu$, $\nu = 9.43$ GHz, γ is the gyromagnetic ratio) is equal to 334 mT. The resonance fields B_r of the resonance signal in the low temperature region (Fig. 3b) have lower values throughout the whole temperature range. This means that for this phase the ferromagnetic coupling is observed according to the relation:

$$(1) \qquad B_{res} = \omega/\gamma - B_A$$

where B_A is the internal anisotropy field.

The paramagnetic state in which $B_s = \omega/\gamma$ was not detected throughout the whole temperature range (see Fig. 3).

In paper [4], the antiferromagnetic state was observed at temperature 180 K for $Ni_{49.1}Mn_{35.4}In_{15.5}$. Such a state results in splitting the resonance signal into two components, according to:

$$(2) \qquad B_{res} = \omega/\gamma \pm [B_A (2B_E + B_A)]^{1/2}$$

where B_E is the exchange field, which couples antiferromagnetic sublattices.

The positive (+) component of the antiferromagnetic resonance signal is observed at temperatures 335–280 K. Below 280 K, the line goes toward the low magnetic field, due to ferromagnetic interaction.
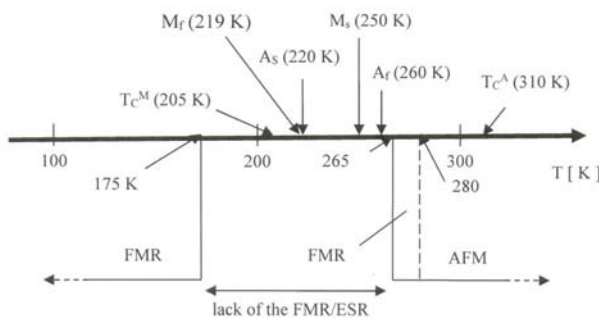
In the mixed state (ferromagnetic and antiferromagnetic), three components of the signal should be observed. However, in our measurements, we did not observe such a case. The FMR intensity of the signals was calculated as:

$$(3) \qquad I_{FMR} = I(\Delta B)^2$$

The temperature dependence of I_{FMR} is shown in Fig. 5.

Austenitic region (335–260 K)

In this range of temperatures, the resonance field is constant in the temperature period of 335 K, up to the temperature 280 K (see Fig. 3). Then, the resonance field decreases linearly with temperature, as for ferromagnetic state. The behavior of the resonance linewidth ΔB vs. temperature is opposite: first, the width decreases linearly from 335 K up to 300 K, and then increases exponentially, up to 265 K.

The FMR intensity I_{FMR} increases almost linearly, starting from the high temperature 335 K, up to $T_C^A = 310$ K. Then, it suddenly drops. In the temperature range 300–305 K, it takes a minimal value. At 295 K, a sudden increase in I_{FMR} is observed, up to the maximum value at 285 K. Then, it decreases with decreasing temperature. Such behavior is still above $M_s = 250$ K.

Martensitic region (175–100 K)

The temperature dependence of the linewidth ΔB in this region of temperatures is similar to the high temperature region. There is a minimum of the dependence $\Delta B(T)$, which is between 145 and 155 K (Fig. 3b). This is far below the characteristic temperatures M_s, M_f, A_s, A_f depicted in Fig. 4. The intensity $I = A + B$ is almost constant in this region. The integrated intensity I_{FMR} increases slowly from 175 K up to 150 K (Fig. 5b). Any further decrease in the temperature results in a quick linear increase of I_{FMR}. The dependence of the resonance field on the temperature shows a maximal value at 155 K.
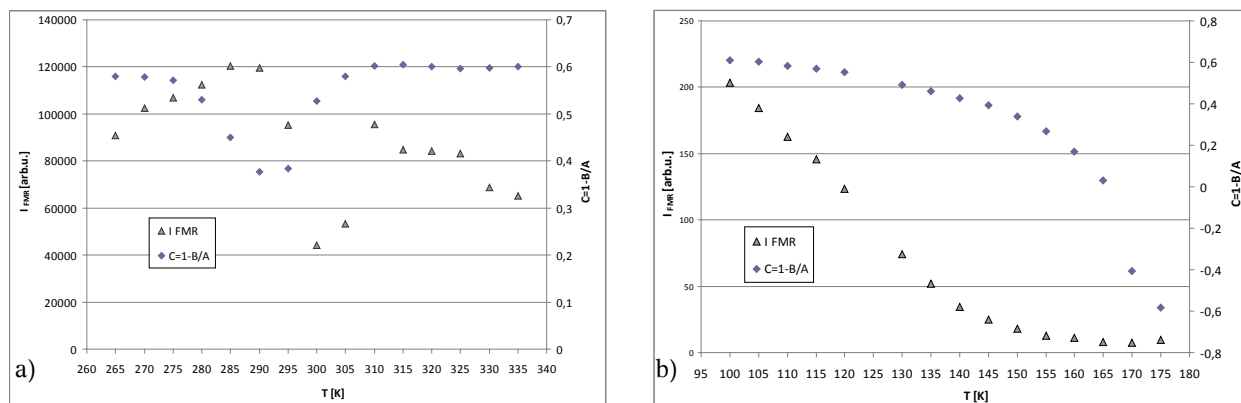

Fig. 4. Characteristic structural and magnetic transition temperatures of $Ni_{49.1}Mn_{35.4}In_{15.5}$ and the range of temperatures in which resonance signal disappear. The data showed in upper part of figure (above the T axes) are taken from Ref. [4].

Fig. 5. Temperature dependence of I_{FMR} and asymmetry parameter $C = 1 - B/A$ for two regions of temperature.

Conclusion

The ferromagnetic and antiferromagnetic resonance in a $Ni_{50}Mn_{35.5}In_{14.5}$ ribbon is observed for the martensitic and austenitic phases separately. In the mixed crystal state (martensite + austenite), the FMR signal disappears.

Below the Curie temperature, in the martensitic state, the essential interaction is ferromagnetic. The temperature dependence of the I_{FMR} differs considerably for the austenitic and martensitic states due to different ferromagnetic ordering.

References

1. Kainuma, R., Imano, Y., Ito, W., Sutou, Y., Morito, H., Okamoto, S., Kitakami, O., Oikawa, K., Fujita, A., Kanomata, T., & Ishida, K. (2006). Magnetic--field-induced shape recovery by reverse phase transformation. *Nature*, *439*, 957–960. DOI: 10.1038/nature04493.
2. Mei, Li, Hu-Bin, Luo, Qing-Miao, Hu, Rui Yang, Chun, Johansson, B., & Vitos, L. (2010). Role of magnetic and atomic ordering in the martensitic transformation of Ni-Mn-In from a first-principles study. *Phys. Rev. B*, *86*, 214205.
3. Aksoy, S., Acet, M., Deen, P. P., Mañosa, L., & Planes, A. (2009). Magnetic correlations in martensitic Ni-Mn-based Heusler shape-memory alloys: Neutron polarization analysis. *Phys. Rev. B*, *79*, 212401.
4. Aksoy, S., Posth, O., Acet, M., Meckenstock, R., Lindner, J., Farle, M., & Wassermann, E. F. (2010). Ferromagnetic resonance in Ni-Mn based ferromagnetic Heusler alloys. *J. Phys.-Conf. Ser.*, *200*, 092001.
5. Rosa, W. O., González, L., García, J., Sánchez, T., Vega, V., Escoda, Ll., Suñol, J. J., Santos, J. D., Alves, M. J. P., Sommer, R. L., Prida, V. M., & Hernando, B. (2012). Tailoring of magnetocaloric effect in $Ni_{45.5}Mn_{43.0}In_{11.5}$ metamagnetic shape memory alloy. *Phys. Res. Int.*, ID795171, 5pp.
6. Pecharsky, V. K., Gschneidner, K. A. Jr, Pecharsky, A. O., & Tishin, A. M. (2001). Thermodynamics of the magnetocaloric effect. *Phys. Rev. B*, *64*, 144406.
7. Ito, W., Imano, Y., Kainuma, R., Suoto, Y., Oikawa, K., & Ishida, K. (2007). Martensitic and magnetic transformation behaviors in Heusler-type NiMnIn and NiCoMnIn metamagnetic shape memory alloys. *Metall. Mater. Trans. A-Phys. Metall. Mater. Sci.*, *38*(4), 759–769.
8. Xu, X., Kihara, T., Tokunaga, M., Matsuo, A., Ito, W., Umetsu, R. Y., Kindo, K., & Kainuma, R. (2013). Magnetic field hysteresis under various sweeping rates for Ni-Co-Mn-In metamagnetic shape memory alloys, magnetic field induced transformation strain in kinetically arrested NiCoMn. *Appl. Phys. Lett.*, *103*(12), 122406(4 pp.).
9. Xuan, C., Chen, F. H., Han, P. D., Wang, D. H., Duc, Y. W. (2014). Effect of Co addition on the martensitic transformation and magnetocaloric effect of Ni-Mn-Al ferromagnetic shape memory alloys. *Intermetallics*, *47*, 31–35.
10. Maziarz, W. (2012). SEM and TEM studies of magnetic shape memory NiCoMnIn melt spun ribbons. *Solid State Phenom.*, *186*, 251–254.
11. Maziarz, W., Czaja, P., Szczerba, M. J., Przewoźnik, J., Kapusta, C., Żywczak, A., Stobiecki, T., Cesari, E., & Dutkiewicz, J. (2013). Room temperature magnetostructural transition in Al for Sn substituted Ni-Mn-Sn melt spun ribbons. *J. Magn. Magn. Mater.*, *348*, 8–16.